FRAMATOME ANP

CALCULATION SUMMARY SHEET (CSS)

Document Identifier 32 - 5019398 - 01

Title PB-1 CRDM NOZZLE IDTB WELD ANOMALY FLAW EVALUATIONS

PREPARED BY:

NAME D.E. KILLIAN

SIGNATURE

TITLE ADVISORY ENGR. DATE 2/26/03

COST CENTER 41629 REF. PAGE(S) 49,50

REVIEWED BY:

METHOD: ☒ DETAILED CHECK ☐ INDEPENDENT CALCULATION

NAME H.P. GUNAWARDANE

SIGNATURE

TITLE ENGINEER II DATE 2/28/03

TM STATEMENT: REVIEWER INDEPENDENCE

PURPOSE AND SUMMARY OF RESULTS:

Revision 1: This revision is a non-proprietary version of Revision 0.

The purpose of this analysis is to perform a fracture mechanics evaluation of a postulated weld anomaly in the Point Beach Unit 1 CRDM nozzle ID temper bead weld repair. The postulated anomaly is a [ ] inch semi-circular flaw extending 360 degrees around the circumference at the "triple point" location where there is a confluence of three materials; the Alloy 600 nozzle, the Alloy [ ] weld, and the low alloy steel head. The anomaly is assumed to propagate in each of two directions on the uphill and downhill sides of the nozzle. The analysis predicts fatigue crack growth in an air environment since the anomaly is located on the outside surface of the new weld, just below the bottom of the severed CRDM tube. Flaw acceptance is based on the 1998 with 2000 Addenda ASME Code Section XI criteria for applied stress intensity factor (IWB-3612) and limit load (IWB-3642).

The results of the analysis demonstrate that a [ ] inch weld anomaly is acceptable for a 25 year design life for the CRDM nozzle ID temper bead weld repair. Significant fracture toughness margins have been demonstrated for each of the two flaw propagation paths considered in the analysis. The minimum fracture toughness margin is 9.57, compared to the required margin of $\sqrt{10}$ per IWB-3612. Fatigue crack growth is minimal. The maximum final flaw size is [ ] inch. The margin on limit load is 8.47, compared to the required margin of 3.0 per IWB-3642.

THE FOLLOWING COMPUTER CODES HAVE BEEN USED IN THIS DOCUMENT:

CODE/VERSION/REV	CODE/VERSION/REV

THE DOCUMENT CONTAINS ASSUMPTIONS THAT MUST BE VERIFIED PRIOR TO USE ON SAFETY-RELATED WORK

☐ YES ☒ NO

RECORD OF REVISIONS

Revision	Affected Pages	Description	Date
0	All	Original release	9/02
1	All	Revision 1 is a non-proprietary version of Revision 0.	2/03

TABLE OF CONTENTS

1.0 INTRODUCTION

The CRDM nozzle ID temper bead weld repair is described by the design drawing (Reference 1). This weld repair establishes a new pressure boundary above the original J-groove weld, except in some cases away from the center of the head where the new weld partially overlaps the original weld. There are seven steps involved in the repair design, as depicted in Reference 1. These steps are:

1) Thermal sleeve cutting
2) Roll expansion
3) Nozzle removal and weld prep machining
4) Welding
5) Grinding/machining and NDE
6) Original weld grinding
7) Thermal sleeve re-attachment

During the welding process (step 4), a maximum [ ] inch weld anomaly may be formed due to lack of fusion at the "triple point", as shown in Figure 1. The anomaly is conservatively assumed to be a "crack-like" defect, 360 degrees around the circumference at the "triple point" location. The technical requirements document (Reference 2) provides additional details of the ID temper bead weld repair procedure. The purpose of the present fracture mechanics analysis is to provide justification, in accordance with Section XI of the ASME Code (Reference 3), for operating with the postulated weld anomaly at the triple point. Predictions of fatigue crack growth are based on a design life of 25 years.

2.0 ASSUMPTIONS

Listed below are assumptions that are pertinent to the present fracture mechanics evaluation.

1) The anomaly is assumed to include a "crack-like" defect, located at the triple-point location and extending all the way around the circumference. For analytical purposes, a continuous circumferential flaw is located in the horizontal plane at the top of the weld. Another continuous flaw is located in the cylindrical plane between the weld and reactor vessel (RV) head.

2) In the radial plane, the anomaly is assumed to include a quarter-circular "crack-like" defect (see Figure 1). For analytical purposes, a semi-circular flaw is used to represent the radial cross-section of the anomaly.

3) It is assumed that the weld residual stresses due to the new repair weld are negligible and therefore can be neglected in the present analysis, as discussed in Reference 5.

4) An RT_{NDT} value of 60 °F is conservatively assumed for the [ ] low alloy reactor vessel head material. This value is commonly used to conservatively represent low alloy ferritic steels.

3.0 WELD ANOMALY

The anomaly is located in the triple point region as shown in Figure 1 below.

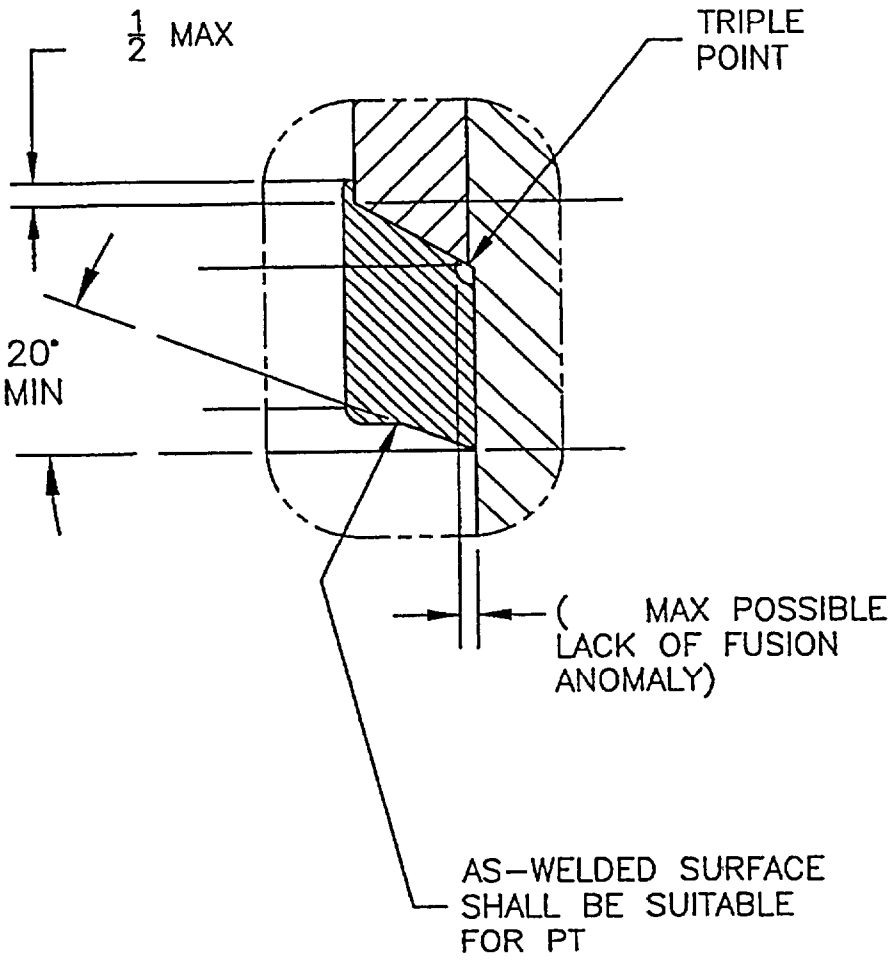

Figure 1. Weld Anomaly in Temper Bead Weld Repair

The region is called a "triple point" since three materials intersect at this location. The materials are:

a) the alloy 600 CRDM nozzle material,

b) the new [ ] filler weld material,* and

c) the low alloy steel RV head material.

* Per Reference 7, Specification 5.14, Par. A7.4.3, "Filler metal of this classification is used for welding nickel-chromium-iron alloy (ASTM B163, B166, B167, and B168 having UNS Number [ ])." This UNS number is associated with Alloy [ ] material.

3.1 Postulated Flaw

The triple point weld anomaly is assumed to be semi-circular in shape with an initial radius of [ ], as indicated in Figure 1. It is further assumed that the anomaly extends 360° around the nozzle. Three flaws are postulated to simulate various orientations and propagation directions for the anomaly. A circumferential flaw and an axial flaw on the outside surface of nozzle would both propagate in a horizontal direction toward the inside surface. A cylindrically oriented flaw along the interface between the weld and head would propagate downward between the two components. The horizontal and vertical flaw propagation directions are represented in Figure 2 by separate paths for the downhill and uphill sides of the nozzle, as discussed below. For both these directions, fatigue crack growth will be calculated considering the most susceptible material for flaw propagation.

Horizontal Direction (Paths 1 and 2):

Flaw propagation is across the CRDM tube wall thickness from the OD of the tube to the ID of the tube. This is the shortest path through the component wall, passing through the new Alloy [ ] weld material. However, Alloy 600 tube material properties or equivalent are used to ensure that another potential path through the HAZ between the new repair weld and the Alloy 600 tube material is bounded.

For completeness, two types of flaws are postulated at the outside surface of the tube. A 360° continuous circumferential flaw, lying in a horizontal plane, is considered to be a conservative representation of crack-like defects that may exist in the weld anomaly. This flaw would be subjected to axial stresses in the tube. An axially oriented semi-circular outside surface flaw is also considered since it would lie in a plane that is normal to the higher circumferential stresses. Both of these flaws would propagate toward the inside surface of the tube.

Vertical Direction (Paths 3 and 4):

Flaw propagation is down the outside surface of the repair weld between the weld and RV head. A continuous surface flaw is postulated to lie along this cylindrical interface between the two materials. This flaw, driven by radial stresses, may propagate along either the new Alloy [ ] weld material or the low alloy steel head material.

4.0 MATERIAL PROPERTIES

The region of interest for the present flaw evaluations is at the triple point, where three different materials intersect. These materials are the CRDM nozzle material, the new weld material and the reactor vessel head material.

The Point Beach Unit 1 CRDM nozzles are made from Alloy 600 material to ASME specification SB-167 for tubular products (Reference 2). The new weld, as noted in Section 3.0, is made from Alloy [ ] type material. The portion of the reactor vessel head that contains the CRDM nozzles is fabricated from [ ] (Reference 2).

4.1 Yield Strength

Values of yield strength, S_y, are obtained from the 1989 Edition of the ASME Code (Reference 9), as listed below.

[ ] Low Alloy Steel Plate Material (RV Head)

Room temperature	50.0 ksi
Operating temperature of 600 °F	43.8 ksi

SB-163 Material [ ] (used for Alloy [ ] Weld Metal)

Room temperature	40.0 ksi
Operating temperature of 600 °F	31.1 ksi

SB-167 Material N06600 (Alloy 600 Material)

Room temperature	35.0 ksi
Operating temperature of 600 °F	27.9 ksi

4.2 Fracture Toughness

4.2.1. Low Alloy Steel RV Head Material

The fracture toughness curve in Figure A-4200-1 of Reference 3 will be used for [ ] material. This curve is specifically applicable to SA-533 Grade B Class 1 plate material and SA-508 Class 2 and 3 forging material [3]. Welding Research Council Bulletin 175 [4] states that this curve may also be used for other steels as long as the specified minimum yield strength does not exceed 50 ksi. It is therefore appropriate to use the Section XI curve to represent the fracture toughness of the Point Beach Unit 1 [ ] reactor vessel head.

At an operating temperature of about 600 °F, the K_{Ia} fracture toughness value for this material (using an assumed RT_{NDT} of 60 °F) is above 200 ksi$\sqrt{in}$. An upper bound value of 200 ksi$\sqrt{in}$ will be conservatively used for the present flaw evaluations.

4.2.2. Alloy 600 and Alloy [ ] Materials

In Table 7 of Reference 12, Mills provides fracture toughness data for unirradiated Alloy 600 material at 24 °C (75 °F) and 427 °C (800 °F) in the form of crack initiation values for the J-integral, J_c. Using linear interpolation and the LEFM plane strain relationship between J_c and fracture toughness, K_{Jc},

$$K_{Jc} = \sqrt{\frac{J_c E}{1-\nu^2}},$$

the fracture toughness at an operating temperature of 600 °F is derived as follows:

Note: $\nu = 0.3$
1 kN/m = 1 kN/m ÷ 4.448 N/lb × 0.0254 m/in = 0.00571 kip/in

Temp. (F)	Mills [12] J_c (kN/m)	J_c (kip/in)	Code [9] E (ksi)	K_{Jc} (ksi$\sqrt{in}$)
75	382	2.18	31000	273
600	522	2.98	28700	307
800	575	3.28	27600	316

Since brittle fracture is not a credible failure mechanism for ductile materials like Alloy 600 or Alloy [ ], these fracture toughness measures, provided for information only, are not considered in the present flaw evaluations. However it should be noted that the fracture toughness measures of these ductile materials is significantly greater than the fracture toughness measure of the low alloy RV head material reported in Section 4.2.1.

4.3 Fatigue Crack Growth

Flaw growth due to fatigue is characterized by

$$\frac{da}{dN} = C_o(\Delta K_I)^n ,$$

where C_o and n are constants that depend on the material and environmental conditions, ΔK_I is the range of applied stress intensity factor in terms of ksi$\sqrt{in}$, and da/dN is the incremental flaw growth in terms of inches/cycle. For the embedded weld anomaly considered in the present analysis, it is appropriate to use crack growth rates for an air environment. Fatigue crack growth is also dependent on the ratio of the minimum to the maximum stress intensity factor; i.e.,

$$R = (K_I)_{min} / (K_I)_{max}$$

[ ] Low Alloy Steel Plate Material (RV Head)

From Article A-4300 of the 1998 Edition of Section XI with addenda through 2000 (Reference 3), the fatigue crack growth constants for subsurface flaws in an air environment are:

$$n = 3.07$$

$$C_o = 1.99 \times 10^{-10} S$$

where $S = 25.72 (2.88 - R)^{-3.07}$ for $0 \le R \le 1$

Alloy 600 and Alloy [ ] Materials (used for Alloy [ ] Weld Metal)

Fatigue crack growth rates for austenitic stainless steels are used to predict flaw growth in the these nickel-chromium-iron components. From Article C-3210 of the 1998 Edition of Section XI with addenda through 2000 (Reference 3), the fatigue crack growth constants for subsurface flaws in an air environment are:

$$n = 3.3$$

$$C_o = C \times S$$

where $C = 10^{[\,-10.009 + 8.12E\text{-}4 \times T - 1.13E\text{-}6 \times T^2 + 1.02E\text{-}9 \times T^3\,]}$

$S = 1.0$ for $R \le 0$

$= 1.0 + 1.8R$ for $0 < R \le 0.79$

$= -43.35 + 57.97R$ for $0.79 < R < 1.0$

5.0 APPLIED STRESSES

The applied stresses are the cyclic stresses that contribute to fatigue crack growth. Fatigue stresses are obtained from a CRDM temper bead design stress analysis (Reference 6) that considered seven transient loading conditions:

Stress Table	Transient	Occurrences in 40 years
1	Heatup and Cooldown	200 cycles
2	Plant Loading and Unloading	3,000 cycles*
3	10% Step Load Changes	2,000 cycles
4	50% Step Load Reduction	200 cycles
5	Reactor Trip	400 cycles
6	Loss of Flow	80 cycles
7	Loss of Load	80 cycles

* Based on a realistic estimate of plant loading and unloading cycles for a non-load following plant.

To simplify the present flaw evaluations while minimizing conservatism, these transients will be grouped into three sets, as listed below. The bounding stresses for the remaining transients (after heatup/cooldown and plant loading/unloading) will be used to conservatively represent these additional cyclic loads.

Group	Transient	Cycles / 40 Years	Cycles / Year
1	Heatup and Cooldown	200	5
2	Plant Loading and Unloading	3,000	75
3	Remaining Transients	2,760	69

Stresses are available from Reference 6 for the four crack propagation paths illustrated in Figure 2. Paths 1 and 3 are located on the downhill (0°) side of the nozzle and Paths 2 and 4 are on the uphill (180°) side. Stresses are reported in a cylindrical coordinate system relative to the CRDM nozzle and include the three component directions (axial, hoop and radial) needed to calculate mode I stress intensity factors for the various postulated flaws. Stresses are provided at four uniform increments along each propagation path.

The length of Paths 1 and 2 is 0.5195" and the lengths of Paths 3 and 4 are 1.4513" (downhill side) and 0.9814" (uphill side), respectively. These path lengths are from a finite element model of an earlier design where the inside surface of the weld was remediated. The horizontal distance between the triple point and the machined weld surface in the present design is

([ ]" – [ ]") / 2 = 0.591" (Reference 1)

Since the actual weld thickness is greater than the analyzed thickness, it is conservative to use the Reference 6 stresses in the present flaw evaluations.

The "vertical" propagation paths extend from the triple point location to the lower portion of the weld at the surface of the enlarged ([ ]") bore. As such, the line is slightly offset from the vertical. It may still be used, however, to represent stresses along this potential propagation path between the weld and head. On the downhill side, Path 3 extends all the way to the bottom of the weld. On the uphill side, Path 4 extends only to the top of the J-groove weld prep (top of butter) since no credit is taken for the integrity of the new-to-old weld overlap in the structural model.

Since stresses are generally higher on the uphill side of the nozzle and the length of Path 4 is less than Path 3 (smaller distance to form a potential leak path), the stresses for Paths 2 and 4 will be used to evaluate postulated flaws at the triple point weld anomaly.

This figure is not pertinent to this document.
2/26/03
(for legibility concerns)

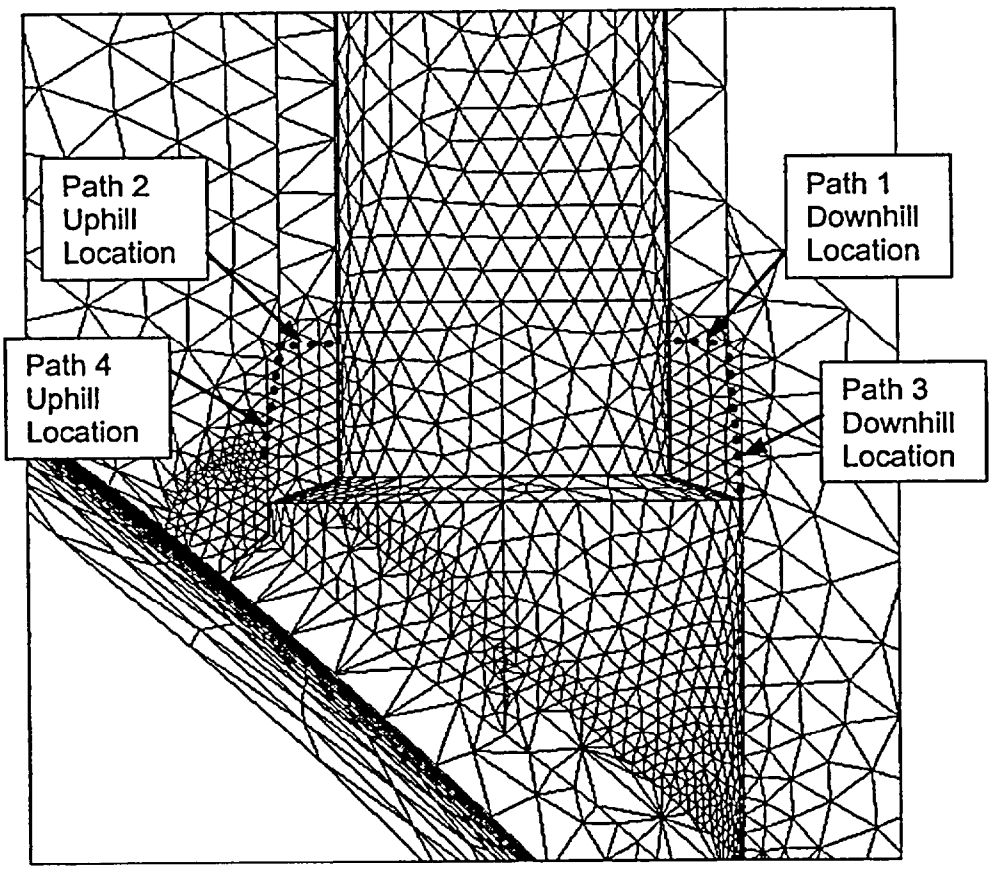

Figure 2. Illustration of Crack Propagation Paths on the Finite Element Stress Model

Table 1. Stresses for Heatup and Cooldown (from Reference 6)

Horizontal Flaw Propagation Paths — Triple Point Location

Path No: PATH1 Length= 0.51953															
Location:	0.0	0.0	0.0	0.12988	0.12988	0.12988	0.25976	0.25976	0.25976	0.38965	0.38965	0.38965	0.51953	0.51953	0.51953
Time	--SX--	--SY--	--SZ--	--SX--	--SY--	--SZ--	--SX--	--SY--	--SZ--	--SX--	--SY--	--SZ--	--SX--	--SY--	--SZ--
1 0.001															
2 2															
3 4.4															
4 6															
5 7.8549															
6 8.6															
7 10.4															
Path No: PATH2 Length= 0.51953															
Location:	0.0	0.0	0.0	0.12988	0.12988	0.12988	0.25976	0.25976	0.25976	0.38965	0.38965	0.38965	0.51953	0.51953	0.51953
Time	--SX--	--SY--	--SZ--	--SX--	--SY--	--SZ--	--SX--	--SY--	--SZ--	--SX--	--SY--	--SZ--	--SX--	--SY--	--SZ--
1 0.001															
2 2															
3 4.4															
4 6															
5 7.8549															
6 8.6															
7 10.4															

Triple Point Location — Vertical Flaw Propagation Paths

Path No: PATH3 Length= 1.4513															
Location:	0.0	0.0	0.0	0.36283	0.36283	0.36283	0.72565	0.72565	0.72565	1.0885	1.0885	1.0885	1.4513	1.4513	1.4513
Time	--SX--	--SY--	--SZ--	--SX--	--SY--	--SZ--	--SX--	--SY--	--SZ--	--SX--	--SY--	--SZ--	--SX--	--SY--	--SZ--
1 0.001															
2 2															
3 4.4															
4 6															
5 7.8549															
6 8.6															
7 10.4															
Path No: PATH4 Length= 0.98139															
Location:	0.0	0.0	0.0	0.24535	0.24535	0.24535	0.4907	0.4907	0.4907	0.73604	0.73604	0.73604	0.98139	0.98139	0.98139
Time	--SX--	--SY--	--SZ--	--SX--	--SY--	--SZ--	--SX--	--SY--	--SZ--	--SX--	--SY--	--SZ--	--SX--	--SY--	--SZ--
1 0.001															
2 2															
3 4.4															
4 6															
5 7.8549															
6 8.6															
7 10.4															

Legend for stress indicators: SX = radial stress SY = hoop stress SZ = axial stress

Table 2. Stresses for Plant Loading and Unloading (from Reference 6)

Horizontal Flaw Propagation Paths — Triple Point Location

Path No: PATH1	Length= 0.51953														
Location:	0.0	0.0	0.0	0.12988	0.12988	0.12988	0.25976	0.25976	0.25976	0.38965	0.38965	0.38965	0.51953	0.51953	0.51953
Time	--SX--	--SY--	--SZ--	--SX--	--SY--	--SZ--	--SX--	--SY--	--SZ--	--SX--	--SY--	--SZ--	--SX--	--SY--	--SZ--
1 0.001															
2 0.3333															
3 3															
4 3.3333															

Path No: PATH2	Length= 0.51953														
Location:	0.0	0.0	0.0	0.12988	0.12988	0.12988	0.25976	0.25976	0.25976	0.38965	0.38965	0.38965	0.51953	0.51953	0.51953
Time	--SX--	--SY--	--SZ--	--SX--	--SY--	--SZ--	--SX--	--SY--	--SZ--	--SX--	--SY--	--SZ--	--SX--	--SY--	--SZ--
1 0.001															
2 0.3333															
3 3															
4 3.3333															

Triple Point Location — Vertical Flaw Propagation Paths

Path No: PATH3	Length= 1.4513														
Location:	0.0	0.0	0.0	0.36283	0.36283	0.36283	0.72565	0.72565	0.72565	1.0885	1.0885	1.0885	1.4513	1.4513	1.4513
Time	--SX--	--SY--	--SZ--	--SX--	--SY--	--SZ--	--SX--	--SY--	--SZ--	--SX--	--SY--	--SZ--	--SX--	--SY--	--SZ--
1 0.001															
2 0.3333															
3 3															
4 3.3333															

Path No: PATH4	Length= 0.98139														
Location:	0.0	0.0	0.0	0.24535	0.24535	0.24535	0.4907	0.4907	0.4907	0.73604	0.73604	0.73604	0.98139	0.98139	0.98139
Time	--SX--	--SY--	--SZ--	--SX--	--SY--	--SZ--	--SX--	--SY--	--SZ--	--SX--	--SY--	--SZ--	--SX--	--SY--	--SZ--
1 0.001															
2 0.3333															
3 3															
4 3.3333															

Legend for stress indicators: SX = radial stress
SY = hoop stress
SZ = axial stress

Table 3. Stresses for 10% Step Load Changes (from Reference 6)

Horizontal Flaw Propagation Paths — Triple Point Location

Path No: PATH1 Length= 0.51953															
Location:	0.0	0.0	0.0	0.12988	0.12988	0.12988	0.25976	0.25976	0.25976	0.38965	0.38965	0.38965	0.51953	0.51953	0.51953
Time	--SX--	--SY--	--SZ--	--SX--	--SY--	--SZ--	--SX--	--SY--	--SZ--	--SX--	--SY--	--SZ--	--SX--	--SY--	--SZ--
1 0.001															
2 0.027778															
3 0.0625															
4 1															
5 1.025															

Path No: PATH2 Length= 0.51953															
Location:	0.0	0.0	0.0	0.12988	0.12988	0.12988	0.25976	0.25976	0.25976	0.38965	0.38965	0.38965	0.51953	0.51953	0.51953
Time	--SX--	--SY--	--SZ--	--SX--	--SY--	--SZ--	--SX--	--SY--	--SZ--	--SX--	--SY--	--SZ--	--SX--	--SY--	--SZ--
1 0.001															
2 0.027778															
3 0.0625															
4 1															
5 1.025															

Vertical Flaw Propagation Paths — Triple Point Location

Path No: PATH3 Length= 1.4513															
Location:	0.0	0.0	0.0	0.36283	0.36283	0.36283	0.72565	0.72565	0.72565	1.0885	1.0885	1.0885	1.4513	1.4513	1.4513
Time	--SX--	--SY--	--SZ--	--SX--	--SY--	--SZ--	--SX--	--SY--	--SZ--	--SX--	--SY--	--SZ--	--SX--	--SY--	--SZ--
1 0.001															
2 0.027778															
3 0.0625															
4 1															
5 1.025															

Path No: PATH4 Length= 0.98139															
Location:	0.0	0.0	0.0	0.24535	0.24535	0.24535	0.4907	0.4907	0.4907	0.73604	0.73604	0.73604	0.98139	0.98139	0.98139
Time	--SX--	--SY--	--SZ--	--SX--	--SY--	--SZ--	--SX--	--SY--	--SZ--	--SX--	--SY--	--SZ--	--SX--	--SY--	--SZ--
1 0.001															
2 0.027778															
3 0.0625															
4 1															
5 1.025															

Legend for stress indicators: SX = radial stress
SY = hoop stress
SZ = axial stress

Table 4. Stresses for 50% Step Load Reduction (from Reference 6)

Horizontal Flaw Propagation Paths — Triple Point Location

Path No: PATH1 Length= 0.51953															
Location:	0.0	0.0	0.0	0.12988	0.12988	0.12988	0.25976	0.25976	0.25976	0.38965	0.38965	0.38965	0.51953	0.51953	0.51953
Time	--SX--	--SY--	--SZ--	--SX--	--SY--	--SZ--	--SX--	--SY--	--SZ--	--SX--	--SY--	--SZ--	--SX--	--SY--	--SZ--
1 0.001															
2 0.05															
3 0.23333															
Path No: PATH2 Length= 0.51953															
Location:	0.0	0.0	0.0	0.12988	0.12988	0.12988	0.25976	0.25976	0.25976	0.38965	0.38965	0.38965	0.51953	0.51953	0.51953
Time	--SX--	--SY--	--SZ--	--SX--	--SY--	--SZ--	--SX--	--SY--	--SZ--	--SX--	--SY--	--SZ--	--SX--	--SY--	--SZ--
1 0.001															
2 0.05															
3 0.23333															

Vertical Flaw Propagation Paths — Triple Point Location

Path No: PATH3 Length= 1.4513															
Location:	0.0	0.0	0.0	0.36283	0.36283	0.36283	0.72565	0.72565	0.72565	1.0885	1.0885	1.0885	1.4513	1.4513	1.4513
Time	--SX--	--SY--	--SZ--	--SX--	--SY--	--SZ--	--SX--	--SY--	--SZ--	--SX--	--SY--	--SZ--	--SX--	--SY--	--SZ--
1 0.001															
2 0.05															
3 0.23333															
Path No: PATH4 Length= 0.98139															
Location:	0.0	0.0	0.0	0.24535	0.24535	0.24535	0.4907	0.4907	0.4907	0.73604	0.73604	0.73604	0.98139	0.98139	0.98139
Time	--SX--	--SY--	--SZ--	--SX--	--SY--	--SZ--	--SX--	--SY--	--SZ--	--SX--	--SY--	--SZ--	--SX--	--SY--	--SZ--
1 0.001															
2 0.05															
3 0.23333															

Legend for stress indicators: SX = radial stress
SY = hoop stress
SZ = axial stress

Table 5. Stresses for Reactor Trip (from Reference 6)

Horizontal Flaw Propagation Paths — Triple Point Location

Path No: PATH1 Length= 0.51953															
Location:	0.0	0.0	0.0	0.12988	0.12988	0.12988	0.25976	0.25976	0.25976	0.38965	0.38965	0.38965	0.51953	0.51953	0.51953
Time	--SX--	--SY--	--SZ--	--SX--	--SY--	--SZ--	--SX--	--SY--	--SZ--	--SX--	--SY--	--SZ--	--SX--	--SY--	--SZ--
1 0.001															
2 0.016667															
3 0.025															

Path No: PATH2 Length= 0.51953															
Location:	0.0	0.0	0.0	0.12988	0.12988	0.12988	0.25976	0.25976	0.25976	0.38965	0.38965	0.38965	0.51953	0.51953	0.51953
Time	--SX--	--SY--	--SZ--	--SX--	--SY--	--SZ--	--SX--	--SY--	--SZ--	--SX--	--SY--	--SZ--	--SX--	--SY--	--SZ--
1 0.001															
2 0.016667															
3 0.025															

Triple Point Location — Vertical Flaw Propagation Paths

Path No: PATH3 Length= 1.4513															
Location:	0.0	0.0	0.0	0.36283	0.36283	0.36283	0.72565	0.72565	0.72565	1.0885	1.0885	1.0885	1.4513	1.4513	1.4513
Time	--SX--	--SY--	--SZ--	--SX--	--SY--	--SZ--	--SX--	--SY--	--SZ--	--SX--	--SY--	--SZ--	--SX--	--SY--	--SZ--
1 0.001															
2 0.016667															
3 0.025															

Path No: PATH4 Length= 0.98139															
Location:	0.0	0.0	0.0	0.24535	0.24535	0.24535	0.4907	0.4907	0.4907	0.73604	0.73604	0.73604	0.98139	0.98139	0.98139
Time	--SX--	--SY--	--SZ--	--SX--	--SY--	--SZ--	--SX--	--SY--	--SZ--	--SX--	--SY--	--SZ--	--SX--	--SY--	--SZ--
1 0.001															
2 0.016667															
3 0.025															

Legend for stress indicators: SX = radial stress
SY = hoop stress
SZ = axial stress

Table 6. Stresses for Loss of Flow (from Reference 6)

Horizontal Flaw Propagation Paths — Triple Point Location

Path No: PATH1	Length= 0.51953														
Location:	0.0	0.0	0.0	0.12988	0.12988	0.12988	0.25976	0.25976	0.25976	0.38965	0.38965	0.38965	0.51953	0.51953	0.51953
Time	--SX--	--SY--	--SZ--	--SX--	--SY--	--SZ--	--SX--	--SY--	--SZ--	--SX--	--SY--	--SZ--	--SX--	--SY--	--SZ--
1 0.001															
2 0.006667															
3 0.04034															

Path No: PATH2	Length= 0.51953														
Location:	0.0	0.0	0.0	0.12988	0.12988	0.12988	0.25976	0.25976	0.25976	0.38965	0.38965	0.38965	0.51953	0.51953	0.51953
Time	--SX--	--SY--	--SZ--	--SX--	--SY--	--SZ--	--SX--	--SY--	--SZ--	--SX--	--SY--	--SZ--	--SX--	--SY--	--SZ--
1 0.001															
2 0.006667															
3 0.04034															

Triple Point Location — Vertical Flaw Propagation Paths

Path No: PATH3	Length= 1.4513														
Location:	0.0	0.0	0.0	0.36283	0.36283	0.36283	0.72565	0.72565	0.72565	1.0885	1.0885	1.0885	1.4513	1.4513	1.4513
Time	--SX--	--SY--	--SZ--	--SX--	--SY--	--SZ--	--SX--	--SY--	--SZ--	--SX--	--SY--	--SZ--	--SX--	--SY--	--SZ--
1 0.001															
2 0.006667															
3 0.04034															

Path No: PATH4	Length= 0.98139														
Location:	0.0	0.0	0.0	0.24535	0.24535	0.24535	0.4907	0.4907	0.4907	0.73604	0.73604	0.73604	0.98139	0.98139	0.98139
Time	--SX--	--SY--	--SZ--	--SX--	--SY--	--SZ--	--SX--	--SY--	--SZ--	--SX--	--SY--	--SZ--	--SX--	--SY--	--SZ--
1 0.001															
2 0.006667															
3 0.04034															

Legend for stress indicators: SX = radial stress
SY = hoop stress
SZ = axial stress

Table 7. Stresses for Loss of Load (from Reference 6)

Horizontal Flaw Propagation Paths — Triple Point Location

Path No: PATH1 Length= 0.51953															
Location:	0.0	0.0	0.0	0.12988	0.12988	0.12988	0.25976	0.25976	0.25976	0.38965	0.38965	0.38965	0.51953	0.51953	0.51953
Time	--SX--	--SY--	--SZ--	--SX--	--SY--	--SZ--	--SX--	--SY--	--SZ--	--SX--	--SY--	--SZ--	--SX--	--SY--	--SZ--
1 0.001															
2 0.002778															
3 0.04444															
Path No: PATH2 Length= 0.51953															
Location:	0.0	0.0	0.0	0.12988	0.12988	0.12988	0.25976	0.25976	0.25976	0.38965	0.38965	0.38965	0.51953	0.51953	0.51953
Time	--SX--	--SY--	--SZ--	--SX--	--SY--	--SZ--	--SX--	--SY--	--SZ--	--SX--	--SY--	--SZ--	--SX--	--SY--	--SZ--
1 0.001															
2 0.002778															
3 0.04444															

Triple Point Location — Vertical Flaw Propagation Paths

Path No: PATH3 Length= 1.4513															
Location:	0.0	0.0	0.0	0.36283	0.36283	0.36283	0.72565	0.72565	0.72565	1.0885	1.0885	1.0885	1.4513	1.4513	1.4513
Time	--SX--	--SY--	--SZ--	--SX--	--SY--	--SZ--	--SX--	--SY--	--SZ--	--SX--	--SY--	--SZ--	--SX--	--SY--	--SZ--
1 0.001															
2 0.002778															
3 0.04444															
Path No: PATH4 Length= 0.98139															
Location:	0.0	0.0	0.0	0.24535	0.24535	0.24535	0.4907	0.4907	0.4907	0.73604	0.73604	0.73604	0.98139	0.98139	0.98139
Time	--SX--	--SY--	--SZ--	--SX--	--SY--	--SZ--	--SX--	--SY--	--SZ--	--SX--	--SY--	--SZ--	--SX--	--SY--	--SZ--
1 0.001															
2 0.002778															
3 0.04444															

Legend for stress indicators: SX = radial stress
SY = hoop stress
SZ = axial stress

6.0 FRACTURE MECHANICS METHODOLOGY

This section presents several aspects of linear elastic fracture mechanics (LEFM) and limit load analysis (to address the ductile Alloy 600 and Alloy [ ] materials) that form the basis of the present flaw evaluations. As discussed in Section 3.1, flaw evaluations are performed for flaw propagation Paths 2 and 4 in Figure 2.

Path 2 represents a section across the new Alloy [ ] weld metal which is equivalent to the thickness of the CRDM tube wall. Since the weld anomaly is located at the base of the OD of the CRDM tube and is assumed to be all the way around the circumference, a stress intensity factor (SIF) solution for a 360 degree circumferential crack on the OD of a circular tube is deemed appropriate. Therefore, the SIF solution of Buchalet and Bamford (Reference 13) is used in the analysis. However, this solution is applicable for a 360-degree part-through ID flaw. To develop an SIF solution for a 360 degree part-through OD flaw, an F function is determined based on SIF solutions of Kumar (References 14 and 15). The appropriate F function for an internal as well as an external circumferential flaw in a cylinder subjected to remote tension are determined first. The ratio of the F functions of the external flaw to the internal flaw is considered to be the appropriate multiplication factor for the Buchalet and Bamford SIF solution, to extend its application to an external crack. The materials to be considered for this path are the Alloy 600 tube material or the Alloy [ ] weld metal. A limit load analysis for an external circumferential flaw in a cylinder subjected to remote tension (Reference 15) is also performed for applied loads on the CRDM tube.

An axially oriented semi-circular OD surface flaw is also considered in the evaluation, as illustrated by the schematic below.

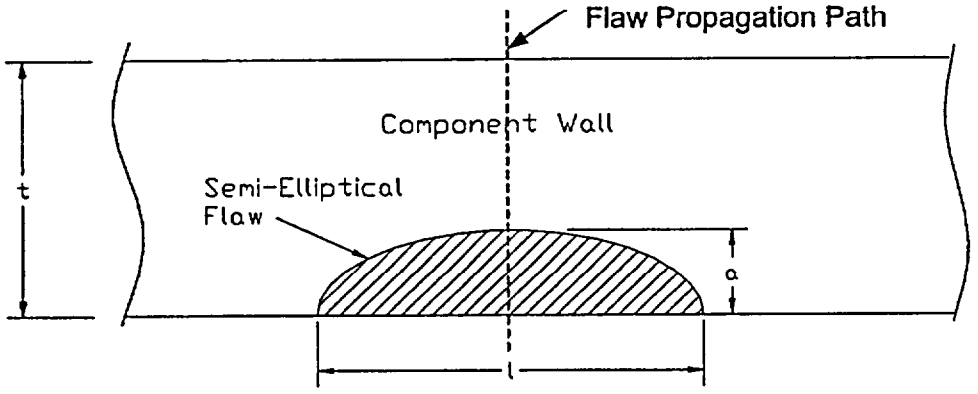

where, a = initial flaw depth = [ ] inch

$l = 2c$ = flaw length = [ ] inch

t = wall thickness = 0.591 inch

An axial flaw is considered since the stresses in the CRDM penetration region are primarily due to pressure and therefore the hoop stresses are more significant. The SIF solution by Raju & Newman (Reference 10) for an external surface crack in a cylindrical vessel is used in the evaluation. The fatigue flaw growth analysis for the axial crack is also performed using the austenitic stainless steel properties.

The Irwin plasticity correction is also considered in the SIF solutions discussed above. This plastic zone correction is discussed in detail in Section 2.8.1 of Reference 11. The effective crack length is defined as the sum of the actual crack size and the plastic zone correction:

$$a_e = a + r_y$$

where r_y for plane strain conditions (applicable for this analysis) is given by:

$$r_y = \frac{1}{6\pi}\left(\frac{K_I}{\sigma_{YS}}\right)^2$$

Path 4 represents the interface between the new repair weld and the RV head material. The potential for flaw propagation along this interface is likely if radial stresses are significant between the weld and head. This assessment utilizes an SIF solution for a continuous surface crack in a flat plate from Appendix A of Section XI (Reference 3). Crack growth analysis is performed considering propagation through the Alloy [ ] weld metal or the low alloy steel head material, whichever is limiting.

7.0 ACCEPTANCE CRITERIA

For low alloy steel materials such as the reactor vessel head material, the evaluation will be performed to the IWB-3612 acceptance criteria of Section XI of the Code (Reference 3). The following considerations are made to address the flaw acceptance criteria for highly ductile materials such as Alloy 600 and Alloy [ ] type materials. The initial flaw depth to thickness ratio for the postulated weld anomaly is about 20%. Fatigue crack growth is minimal for Alloy 600 or Alloy [ ] materials in an air environment. The only acceptance criterion on flaw size is the industry developed 75% through-wall limit on depth (Reference 8):

$$\frac{a}{t} \leq 0.75$$

For the shallow cracks considered in the present analysis, this criterion is easily met.

Another acceptance criterion for ductile materials is demonstration of sufficient limit load margin. From IWB-3642 (Reference 3), the required safety margin, based on load, is a factor of 3 for normal and upset operating conditions. Stress intensity factors are also evaluated considering the required fracture toughness margin of $\sqrt{10}$ for normal and upset operating conditions.

8.0 FLAW EVALUATIONS

The evaluation of the postulated external circumferential flaw for propagation along Path 2 is contained in Tables 8 and 9. The fatigue crack growth analysis is provided in Table 8 and a limit load analysis is presented in Table 9.

The evaluation of an external axial flaw for fatigue crack growth along Path 2 is contained in Table 10.

A continuous surface flaw between the repair weld and the RV head is analyzed for fatigue crack growth along Path 4 in Table 11.

The fatigue crack growth analyses (in Tables 8, 10, and 11) uniformly distribute the applied cycles over the 25 year service life by linking the incremental crack growth due to various loading conditions.

Table 8. Evaluation of Continuous External Circumferential Flaw for Fatigue Crack Growth Along Path 2

INPUT DATA

Geometry:	Outside diameter,	Do =	[ ]	in.
	Inside diameter,	Di =	[ ]	in.
	Thickness,	t =	0.591	in.
		Ri/t =	[ ]	
Flaw Size:	Flaw depth,	a =	[ ]	in.
		a/t =	[ ]	
Environment:	Temperature,	T =	600	F
Material Strength:	Yield strength,	σ_{ys} =	27.9	ksi

Table 8. Evaluation of Continuous External Circumferential Flaw for Fatigue Crack Growth Along Path 2 (Cont'd)

Variation of F Function between Continuous External and Continuous Internal Circumferential Flaws Using Solutions by V. Kumar et al.

Source: EPRI NP-1931 Topical Report, Section 4.3 for F Function for An Internal Circumferential Crack Under Remote Tension (Ref. 14).

The applied KI equation is given by the expression:

$$KI = \sigma * \sqrt{(\pi * a)} * F(a/b, Ri/Ro)$$

where

$$\sigma = P/(\pi * (Ro^2 - Ri^2))$$

and F is a function of a/b and Ri/Ro or b/Ri.

For this application:

a/b = [ ]
b/Ri = [ ]

By extrapolation from Table 4-5 of EPRI-1931, F is estimated to be:

F = 1.11

Source: GE Report SRD-82-048, Prepared for EPRI Contract RP-1237-1, Fifth & Sixth Semi-Annual Report, Section 3.5 for F Function (Ref. 15).

For the external circumferential crack, the expressions for KI and σ are as defined above for the internal circumferential crack.

From Figure 3-11, the F function for:

a/b = [ ]
Ri/Ro = [ ]

is estimated to be,

F = 1.25

Multiplying Factor:

To estimate the stress intensity factor for an external circumferential crack from the solution for an internal circumferential crack under remote tension, the appropriate multiplying factor is: 1.13

Table 8. Evaluation of Continuous External Circumferential Flaw for Fatigue Crack Growth Along Path 2 (Cont'd)

CIRCUMFERENTIAL FLAW STRESS INTENSITY FACTOR FOR HEATUP AND COOLDOWN STRESSES

Basis: Buchalet and Bamford solution for continuous circumferential flaws on the inside surface of cylinders (Ref. 13)

$$KI = \sqrt{(\pi a)} * [\, A_0 F_1 + (2a/\pi) A_1 F_2 + (a^2/2) A_2 F_3 + (4a^3)/(3\pi) A_3 F_4 \,]$$

where,

$$F1 = 1.1259 + 0.2344(a/t) + 2.2018(a/t)^2 - 0.2083(a/t)^3$$
$$F2 = 1.0732 + 0.2677(a/t) + 0.6661(a/t)^2 + 0.6354(a/t)^3$$
$$F3 = 1.0528 + 0.1065(a/t) + 0.4429(a/t)^2 + 0.6042(a/t)^3$$
$$F4 = 1.0387 - 0.0939(a/t) + 0.6018(a/t)^2 + 0.3750(a/t)^3$$

and the through-wall stress distribution is described by the third order polynomial,

$$S(x) = A_0 + A_1 x + A_2 x^2 + A_3 x^3.$$

Applicablility: $R_i/t = 10$
$a/t \leq 0.8$

Axial Stresses:

Wall Position x	Normal/Upset Cond. Stresses [6]	
	SS*	Shutdown
(in.)	(ksi)	(ksi)
0.00000		
0.14775		
0.29550		
0.44325		
0.59100		

* Heatup/Cooldown transient at 6.0 hours (steady state) using stresses for Path 2

Stress Coefficients:

Stress Coeff.	Normal/Upset Loading Conditions	
	NU1	NU2
	(ksi)	(ksi)
A_0		
A_1		
A_2		
A_3		

Table 8. Evaluation of Continuous External Circumferential Flaw for Fatigue Crack Growth Along Path 2 (Cont'd)

CIRCUMFERENTIAL FLAW STRESS INTENSITY FACTOR FOR PLANT LOADING AND UNLOADING STRESSES

Basis: Buchalet and Bamford solution for continuous circumferential flaws on the inside surface of cylinders (Ref. 13)

$$KI = \sqrt{(\pi^* a)} * [\, A_0 F_1 + (2a/\pi) A_1 F_2 + (a^2/2) A_2 F_3 + (4a^3)/(3\pi) A_3 F_4 \,]$$

where,

$$F1 = 1.1259 + 0.2344(a/t) + 2.2018(a/t)^2 - 0.2083(a/t)^3$$
$$F2 = 1.0732 + 0.2677(a/t) + 0.6661(a/t)^2 + 0.6354(a/t)^3$$
$$F3 = 1.0528 + 0.1065(a/t) + 0.4429(a/t)^2 + 0.6042(a/t)^3$$
$$F4 = 1.0387 - 0.0939(a/t) + 0.6018(a/t)^2 + 0.3750(a/t)^3$$

and the through-wall stress distribution is described by the third order polynomial,

$$S(x) = A_0 + A_1 x + A_2 x^2 + A_3 x^3.$$

Applicablility: $R_i/t = 10$
$a/t \leq 0.8$

Axial Stresses:

Wall Position x	Normal/Upset Cond. Stresses [6]	
	PU*	PL**
(in.)	(ksi)	(ksi)
0.00000		
0.14775		
0.29550		
0.44325		
0.59100		

* Plant Loading/Unloading transient at 3.333 hours (plant unloading) using stresses for Path 2

** Plant Loading/Unloading transient at 0.333 hours (plant loading) using stresses for Path 2

Stress Coefficients:

Stress Coeff.	Normal/Upset Loading Conditions	
	NU1	NU2
	(ksi)	(ksi)
A_0		
A_1		
A_2		
A_3		

Table 8. Evaluation of Continuous External Circumferential Flaw for Fatigue Crack Growth Along Path 2 (Cont'd)

CIRCUMFERENTIAL FLAW STRESS INTENSITY FACTOR FOR REMAINING TRANSIENT STRESSES

Basis: Buchalet and Bamford solution for continuous circumferential flaws on the inside surface of cylinders (Ref. 13)

$$KI = \sqrt{(\pi a)} * [\, A_0 F_1 + (2a/\pi) A_1 F_2 + (a^2/2) A_2 F_3 + (4a^3)/(3\pi) A_3 F_4 \,]$$

where,

$$F1 = 1.1259 + 0.2344(a/t) + 2.2018(a/t)^2 - 0.2083(a/t)^3$$
$$F2 = 1.0732 + 0.2677(a/t) + 0.6661(a/t)^2 + 0.6354(a/t)^3$$
$$F3 = 1.0528 + 0.1065(a/t) + 0.4429(a/t)^2 + 0.6042(a/t)^3$$
$$F4 = 1.0387 - 0.0939(a/t) + 0.6018(a/t)^2 + 0.3750(a/t)^3$$

and the through-wall stress distribution is described by the third order polynomial,

$$S(x) = A_0 + A_1 x + A_2 x^2 + A_3 x^3.$$

Applicablility: Ri/t = 10
a/t ≤ 0.8

Axial Stresses:

Wall Position x	Normal/Upset Cond. Stresses [6]	
	LL1*	LL2**
(in.)	(ksi)	(ksi)
0.00000		
0.14775		
0.29550		
0.44325		
0.59100		

* Loss of Load transient at 0.00278 hours (max. stress) using stresses for Path 2

** Loss of Load transient at 0.0444 hours (min. stress) using stresses for Path 2

Stress Coefficients:

Stress Coeff.	Normal/Upset Loading Conditions	
	NU1	NU2
	(ksi)	(ksi)
A_0		
A_1		
A_2		
A_3		

Table 8. Evaluation of Continuous External Circumferential Flaw for Fatigue Crack Growth Along Path 2 (Cont'd)

CIRCUMFERENTIAL FLAW FATIGUE CRACK GROWTH FOR HEATUP AND COOLDOWN TRANSIENT

Basis: $\Delta a = \Delta N * C_o(\Delta KI)^n$

Transient frequency: 200 cycles over 40 years

ΔN = 5 cycles/year

Operating Time (yr.)	Cycle	a (in.)	NU1 KI(a)max (ksi√in)	NU2 KI(a)min (ksi√in)	ΔKI (ksi√in)	R	S	C_o	Δa (in.)	r_y	a_e	NU1 KI(a_e)max (ksi√in)
0	0		15.68	0.00	15.68	0.00	1.00	1.96E-10	8.62E-06	0.017		16.17
1	5		15.69	0.00	15.69	0.00	1.00	1.96E-10	8.63E-06	0.017		16.18
2	10		15.69	0.00	15.69	0.00	1.00	1.96E-10	8.63E-06	0.017		16.18
3	15		15.69	0.00	15.69	0.00	1.00	1.96E-10	8.63E-06	0.017		16.18
4	20		15.69	0.00	15.69	0.00	1.00	1.96E-10	8.63E-06	0.017		16.18
5	25		15.69	0.00	15.69	0.00	1.00	1.96E-10	8.63E-06	0.017		16.18
6	30		15.69	0.00	15.69	0.00	1.00	1.96E-10	8.64E-06	0.017		16.18
7	35		15.69	0.00	15.69	0.00	1.00	1.96E-10	8.64E-06	0.017		16.18
8	40		15.69	0.00	15.69	0.00	1.00	1.96E-10	8.64E-06	0.017		16.18
9	45		15.69	0.00	15.69	0.00	1.00	1.96E-10	8.64E-06	0.017		16.18
10	50		15.69	0.00	15.69	0.00	1.00	1.96E-10	8.64E-06	0.017		16.18
11	55		15.70	0.00	15.70	0.00	1.00	1.96E-10	8.65E-06	0.017		16.18
12	60		15.70	0.00	15.70	0.00	1.00	1.96E-10	8.65E-06	0.017		16.18
13	65		15.70	0.00	15.70	0.00	1.00	1.96E-10	8.65E-06	0.017		16.19
14	70		15.70	0.00	15.70	0.00	1.00	1.96E-10	8.65E-06	0.017		16.19
15	75		15.70	0.00	15.70	0.00	1.00	1.96E-10	8.65E-06	0.017		16.19
16	80		15.70	0.00	15.70	0.00	1.00	1.96E-10	8.65E-06	0.017		16.19
17	85		15.70	0.00	15.70	0.00	1.00	1.96E-10	8.66E-06	0.017		16.19
18	90		15.70	0.00	15.70	0.00	1.00	1.96E-10	8.66E-06	0.017		16.19
19	95		15.70	0.00	15.70	0.00	1.00	1.96E-10	8.66E-06	0.017		16.19
20	100		15.71	0.00	15.71	0.00	1.00	1.96E-10	8.66E-06	0.017		16.19
21	105		15.71	0.00	15.71	0.00	1.00	1.96E-10	8.66E-06	0.017		16.19
22	110		15.71	0.00	15.71	0.00	1.00	1.96E-10	8.67E-06	0.017		16.19
23	115		15.71	0.00	15.71	0.00	1.00	1.96E-10	8.67E-06	0.017		16.19
24	120		15.71	0.00	15.71	0.00	1.00	1.96E-10	8.67E-06	0.017		16.19
25	125		15.71	0.00	15.71	0.00	1.00	1.96E-10	8.67E-06	0.017		16.20

Table 8. Evaluation of Continuous External Circumferential Flaw for Fatigue Crack Growth Along Path 2 (Cont'd)

CIRCUMFERENTIAL FLAW FATIGUE CRACK GROWTH FOR PLANT LOADING AND UNLOADING TRANSIENT

Basis: $\Delta a = \Delta N * C_o(\Delta KI)^n$

Transient frequency: 3000 cycles over 40 years

ΔN = 75 cycles/year

Operating Time (yr.)	Cycle	a (in.)	NU1 KI(a)max (ksi√in)	NU2 KI(a)min (ksi√in)	ΔKI (ksi√in)	R	S	C_o	Δa (in.)	r_y	a_e	NU1 KI(a_e)max (ksi√in)
0	0		15.26	12.38	2.88	0.81	3.68	7.20E-10	1.77E-06	0.016		15.66
1	75		15.26	12.38	2.88	0.81	3.68	7.20E-10	1.77E-06	0.016		15.66
2	150		15.26	12.38	2.88	0.81	3.68	7.20E-10	1.77E-06	0.016		15.67
3	225		15.26	12.38	2.88	0.81	3.68	7.20E-10	1.77E-06	0.016		15.67
4	300		15.26	12.38	2.88	0.81	3.68	7.21E-10	1.77E-06	0.016		15.67
5	375		15.26	12.38	2.88	0.81	3.68	7.21E-10	1.77E-06	0.016		15.67
6	450		15.26	12.38	2.88	0.81	3.68	7.21E-10	1.77E-06	0.016		15.67
7	525		15.26	12.38	2.88	0.81	3.68	7.21E-10	1.77E-06	0.016		15.67
8	600		15.26	12.38	2.88	0.81	3.68	7.21E-10	1.77E-06	0.016		15.67
9	675		15.26	12.38	2.88	0.81	3.68	7.21E-10	1.77E-06	0.016		15.67
10	750		15.27	12.39	2.88	0.81	3.68	7.21E-10	1.77E-06	0.016		15.67
11	825		15.27	12.39	2.88	0.81	3.69	7.21E-10	1.77E-06	0.016		15.67
12	900		15.27	12.39	2.88	0.81	3.69	7.21E-10	1.77E-06	0.016		15.67
13	975		15.27	12.39	2.88	0.81	3.69	7.22E-10	1.78E-06	0.016		15.67
14	1050		15.27	12.39	2.88	0.81	3.69	7.22E-10	1.78E-06	0.016		15.67
15	1125		15.27	12.39	2.88	0.81	3.69	7.22E-10	1.78E-06	0.016		15.67
16	1200		15.27	12.39	2.88	0.81	3.69	7.22E-10	1.78E-06	0.016		15.68
17	1275		15.27	12.39	2.88	0.81	3.69	7.22E-10	1.78E-06	0.016		15.68
18	1350		15.27	12.39	2.88	0.81	3.69	7.22E-10	1.78E-06	0.016		15.68
19	1425		15.27	12.39	2.88	0.81	3.69	7.22E-10	1.78E-06	0.016		15.68
20	1500		15.27	12.39	2.88	0.81	3.69	7.22E-10	1.78E-06	0.016		15.68
21	1575		15.28	12.40	2.88	0.81	3.69	7.22E-10	1.78E-06	0.016		15.68
22	1650		15.28	12.40	2.88	0.81	3.69	7.23E-10	1.78E-06	0.016		15.68
23	1725		15.28	12.40	2.88	0.81	3.69	7.23E-10	1.78E-06	0.016		15.68
24	1800		15.28	12.40	2.88	0.81	3.69	7.23E-10	1.78E-06	0.016		15.68
25	1875		15.28	12.40	2.88	0.81	3.69	7.23E-10	1.78E-06	0.016		15.68

Table 8. Evaluation of Continuous External Circumferential Flaw for Fatigue Crack Growth Along Path 2 (Cont'd)

CIRCUMFERENTIAL FLAW FATIGUE CRACK GROWTH FOR REMAINING TRANSIENTS

Basis: $\Delta a = \Delta N * C_o(\Delta KI)^n$

Transient frequency: 2760 cycles over 40 years

ΔN = 69 cycles/year

Operating Time (yr.)	Cycle	a (in.)	NU1 KI(a)max (ksi√in)	NU2 KI(a)min (ksi√in)	ΔKI (ksi√in)	R	S	C_o	Δa (in.)	r_y	a_e	NU1 KI(a_e)max (ksi√in)
0	0		17.18	9.74	7.45	0.57	2.02	3.95E-10	2.06E-05	0.020		17.86
1	69		17.18	9.74	7.45	0.57	2.02	3.95E-10	2.06E-05	0.020		17.86
2	138		17.19	9.74	7.45	0.57	2.02	3.95E-10	2.06E-05	0.020		17.86
3	207		17.19	9.74	7.45	0.57	2.02	3.95E-10	2.06E-05	0.020		17.86
4	276		17.19	9.74	7.45	0.57	2.02	3.95E-10	2.06E-05	0.020		17.86
5	345		17.19	9.74	7.45	0.57	2.02	3.95E-10	2.06E-05	0.020		17.86
6	414		17.19	9.74	7.45	0.57	2.02	3.95E-10	2.06E-05	0.020		17.86
7	483		17.19	9.74	7.45	0.57	2.02	3.95E-10	2.06E-05	0.020		17.87
8	552		17.19	9.74	7.45	0.57	2.02	3.95E-10	2.06E-05	0.020		17.87
9	621		17.19	9.74	7.45	0.57	2.02	3.95E-10	2.06E-05	0.020		17.87
10	690		17.20	9.74	7.45	0.57	2.02	3.95E-10	2.06E-05	0.020		17.87
11	759		17.20	9.74	7.46	0.57	2.02	3.95E-10	2.07E-05	0.020		17.87
12	828		17.20	9.74	7.46	0.57	2.02	3.95E-10	2.07E-05	0.020		17.87
13	897		17.20	9.74	7.46	0.57	2.02	3.95E-10	2.07E-05	0.020		17.87
14	966		17.20	9.74	7.46	0.57	2.02	3.95E-10	2.07E-05	0.020		17.87
15	1035		17.20	9.74	7.46	0.57	2.02	3.95E-10	2.07E-05	0.020		17.87
16	1104		17.20	9.74	7.46	0.57	2.02	3.95E-10	2.07E-05	0.020		17.87
17	1173		17.20	9.74	7.46	0.57	2.02	3.95E-10	2.07E-05	0.020		17.88
18	1242		17.21	9.74	7.46	0.57	2.02	3.95E-10	2.07E-05	0.020		17.88
19	1311		17.21	9.75	7.46	0.57	2.02	3.95E-10	2.07E-05	0.020		17.88
20	1380		17.21	9.75	7.46	0.57	2.02	3.95E-10	2.07E-05	0.020		17.88
21	1449		17.21	9.75	7.46	0.57	2.02	3.95E-10	2.07E-05	0.020		17.88
22	1518		17.21	9.75	7.46	0.57	2.02	3.95E-10	2.07E-05	0.020		17.88
23	1587		17.21	9.75	7.46	0.57	2.02	3.95E-10	2.07E-05	0.020		17.88
24	1656		17.21	9.75	7.46	0.57	2.02	3.95E-10	2.07E-05	0.020		17.88
25	1725		17.21	9.75	7.46	0.57	2.02	3.95E-10	2.07E-05	0.020		17.88

Table 9. Limit Load Analysis for a Continuous External Circumferenital Flaw

LIMIT LOAD

Basis: GE Report SRD-82-048, Combined Fifth and Sixth Semi-Annual Report by V. Kumar et al, Section 3.5 (Ref. 15).

For remote tension loading,

$$Po = 2/\sqrt{3}*\sigma_o*\pi*(Rc^2-Ri^2)$$

where

$Rc = Ro - a$

and

$\sigma_o =$ 27900 psi (conservatively using the minimum yield strength)

$Ro =$ [ ] in.

$a =$ [ ] in.

$Rc =$ [ ] in.

$Ri =$ [ ] in.

Then

$Po =$ [ ] lbs

A bounding axial tube load on the CRDM tube is the hydrostatic test load:

$$P = (\pi Ri^2)*p_h$$

where

p_h = hydrostatic test pressure

= 1.25 times the design pressure

$p_d =$ [ ] psig (Ref. 2)

Then

$p_h =$ [ ] psig

and

$P =$ [ ] lbs

The limit load safety margin is:

$Po/P =$ 8.47

This safety margin is greater than the value of 3 required by Article IWB-3642 of Section XI (Reference 3).

Table 10. Evaluation of Continuous External Circumferential Flaw for Fatigue Crack Growth Along Path 2

INPUT DATA

Geometry:	Outside diameter,	Do =	[ ]	in.
	Inside diameter,	Di =	[ ]	in.
	Thickness,	t =	0.591	in.
		Ri/t =	[ ]	
Flaw Size:	Flaw depth,	a =	[ ]	in.
		a/t =	[ ]	
Environment:	Temperature,	T =	600	F
Material Strength:	Yield strength,	σ_{ys} =	27.9	ksi

Table 10. Evaluation of an External Axial Flaw for Fatigue Crack Growth Along Path 2

AXIAL FLAW STRESS INTENSITY FACTOR FOR HEATUP AND COOLDOWN STRESSES

Basis: Raju & Newman, "Stress Intensity Factors for Internal & External Surface Cracks in Cylindrical Vessels (Ref. 10)

$$KI = \sqrt{(\pi/Q)} * [G_0 A_0 a^{0.5} + G_1 A_1 a^{1.5} + G_2 A_2 a^{2.5} + G_3 A_3 a^{3.5}]$$

where, per Table 4, for an external surface crack and for t/R = 0.25, a/t = 0.2, $2\phi/\pi = 1$, and a/c = 1.0

Go =	1.030
G_1 =	0.720
G_2 =	0.591
G_3 =	0.513

and **Q =** 2.464 = (1 + 1.464*(a/c)^1.65)

and the through-wall stress distribution is described by the third order polynomial,

$$S(x) = A_0 + A_1 x + A_2 x^2 + A_3 x^3.$$

Hoop Stresses:

Wall Position x	Normal/Upset Cond. Stresses [6]	
	SS*	Shutdown
(in.)	(ksi)	(ksi)
0.00000		
0.14775		
0.29550		
0.44325		
0.59100		

* Heatup/Cooldown transient at 6.0 hours (steady state) using stresses for Path 2

Stress Coefficients:

Stress Coeff.	Normal/Upset Loading Conditions	
	NU1	NU2
	(ksi)	(ksi)
A_0		
A_1		
A_2		
A_3		

Table 10. Evaluation of an External Axial Flaw for Fatigue Crack Growth Along Path 2

AXIAL FLAW STRESS INTENSITY FACTOR FOR PLANT LOADING AND UNLOADING STRESSES

Basis: Raju & Newman, "Stress Intensity Factors for Internal & External Surface Cracks in Cylindrical Vessels (Ref. 10)

$$KI = \sqrt{(\pi/Q)} * [G_0 A_0 a^{0.5} + G_1 A_1 a^{1.5} + G_2 A_2 a^{2.5} + G_3 A_3 a^{3.5}]$$

where, per Table 4, for an external surface crack and for t/R = 0.25, a/t = 0.2, $2\phi/\pi = 1$, and a/c = 1.0

Go = 1.030
G_1 = 0.720
G_2 = 0.591
G_3 = 0.513

and Q = 2.464 = (1 + 1.464*(a/c)^1.65)

and the through-wall stress distribution is described by the third order polynomial,

$$S(x) = A_0 + A_1 x + A_2 x^2 + A_3 x^3.$$

Hoop Stresses:

Wall Position x	Normal/Upset Cond. Stresses [6]	
	PU*	PL**
(in.)	(ksi)	(ksi)
0.00000		
0.14775		
0.29550		
0.44325		
0.59100		

* Plant Loading/Unloading transient at 3.333 hours (plant unloading) using stresses for Path 2

** Plant Loading/Unloading transient at 0.333 hours (plant loading) using stresses for Path 2

Stress Coefficients:

Stress Coeff.	Normal/Upset Loading Conditions	
	NU1	NU2
	(ksi)	(ksi)
A_0		
A_1		
A_2		
A_3		

Table 10. Evaluation of an External Axial Flaw for Fatigue Crack Growth Along Path 2

AXIAL FLAW STRESS INTENSITY FACTOR FOR REMAINING TRANSIENT STRESSES

Basis: Raju & Newman, "Stress Intensity Factors for Internal & External Surface Cracks in Cylindrical Vessels (Ref. 10)

$$KI = \sqrt{(\pi/Q)} * [G_0 A_0 a^{0.5} + G_1 A_1 a^{1.5} + G_2 A_2 a^{2.5} + G_3 A_3 a^{3.5}]$$

where, per Table 4, for an external surface crack and for t/R = 0.25, a/t = 0.2, $2\phi/\pi$ = 1, and a/c = 1.0

G_o = 1.030
G_1 = 0.720
G_2 = 0.591
G_3 = 0.513

and Q = 2.464 = (1 + 1.464*(a/c)^1.65)

and the through-wall stress distribution is described by the third order polynomial,

$$S(x) = A_0 + A_1 x + A_2 x^2 + A_3 x^3.$$

Hoop Stresses:

Wall Position x	Normal/Upset Cond. Stresses [6]	
	LL1*	LL2**
(in.)	(ksi)	(ksi)
0.00000		
0.14775		
0.29550		
0.44325		
0.59100		

* Loss of Load transient at 0.00278 hours (max. stress) using stresses for Path 2

** Loss of Load transient at 0.0444 hours (min. stress) using stresses for Path 2

Stress Coefficients:

Stress Coeff.	Normal/Upset Loading Conditions	
	NU1	NU2
	(ksi)	(ksi)
A_0		
A_1		
A_2		
A_3		

Table 10. Evaluation of an External Axial Flaw for Fatigue Crack Growth Along Path 2 (Cont'd)

AXIAL FLAW FATIGUE CRACK GROWTH FOR HEATUP AND COOLDOWN TRANSIENT

Basis: $\Delta a = \Delta N * C_o(\Delta KI)^n$

Transient frequency: 200 cycles over 40 years

ΔN = 5 cycles/year

Operating Time (yr.)	Cycle	a (in.)	NU1 KI(a)max (ksi√in)	NU2 KI(a)min (ksi√in)	ΔKI (ksi√in)	R	S	C_o	Δa (in.)	r_y	a_e	NU1 KI(a_e)max (ksi√in)
0	0		13.79	0.00	13.79	0.00	1.00	1.96E-10	5.64E-06	0.013		14.44
1	5		13.80	0.00	13.80	0.00	1.00	1.96E-10	5.65E-06	0.013		14.44
2	10		13.80	0.00	13.80	0.00	1.00	1.96E-10	5.65E-06	0.013		14.44
3	15		13.80	0.00	13.80	0.00	1.00	1.96E-10	5.65E-06	0.013		14.44
4	20		13.80	0.00	13.80	0.00	1.00	1.96E-10	5.65E-06	0.013		14.45
5	25		13.80	0.00	13.80	0.00	1.00	1.96E-10	5.65E-06	0.013		14.45
6	30		13.80	0.00	13.80	0.00	1.00	1.96E-10	5.65E-06	0.013		14.45
7	35		13.80	0.00	13.80	0.00	1.00	1.96E-10	5.66E-06	0.013		14.45
8	40		13.80	0.00	13.80	0.00	1.00	1.96E-10	5.66E-06	0.013		14.45
9	45		13.80	0.00	13.80	0.00	1.00	1.96E-10	5.66E-06	0.013		14.45
10	50		13.80	0.00	13.80	0.00	1.00	1.96E-10	5.66E-06	0.013		14.45
11	55		13.81	0.00	13.81	0.00	1.00	1.96E-10	5.66E-06	0.013		14.45
12	60		13.81	0.00	13.81	0.00	1.00	1.96E-10	5.66E-06	0.013		14.45
13	65		13.81	0.00	13.81	0.00	1.00	1.96E-10	5.66E-06	0.013		14.45
14	70		13.81	0.00	13.81	0.00	1.00	1.96E-10	5.67E-06	0.013		14.46
15	75		13.81	0.00	13.81	0.00	1.00	1.96E-10	5.67E-06	0.013		14.46
16	80		13.81	0.00	13.81	0.00	1.00	1.96E-10	5.67E-06	0.013		14.46
17	85		13.81	0.00	13.81	0.00	1.00	1.96E-10	5.67E-06	0.013		14.46
18	90		13.81	0.00	13.81	0.00	1.00	1.96E-10	5.67E-06	0.013		14.46
19	95		13.81	0.00	13.81	0.00	1.00	1.96E-10	5.67E-06	0.013		14.46
20	100		13.82	0.00	13.82	0.00	1.00	1.96E-10	5.67E-06	0.013		14.46
21	105		13.82	0.00	13.82	0.00	1.00	1.96E-10	5.68E-06	0.013		14.46
22	110		13.82	0.00	13.82	0.00	1.00	1.96E-10	5.68E-06	0.013		14.46
23	115		13.82	0.00	13.82	0.00	1.00	1.96E-10	5.68E-06	0.013		14.47
24	120		13.82	0.00	13.82	0.00	1.00	1.96E-10	5.68E-06	0.013		14.47
25	125		13.82	0.00	13.82	0.00	1.00	1.96E-10	5.68E-06	0.013		14.47

Table 10. Evaluation of an External Axial Flaw for Fatigue Crack Growth Along Path 2 (Cont'd)

AXIAL FLAW FATIGUE CRACK GROWTH FOR PLANT LOADING AND UNLOADING TRANSIENT

Basis: $\Delta a = \Delta N * C_o(\Delta KI)^n$

Transient frequency: 3000 cycles over 40 years

ΔN = 75 cycles/year

Operating Time (yr.)	Cycle	a (in.)	NU1 KI(a)max (ksi√in)	NU2 KI(a)min (ksi√in)	ΔKI (ksi√in)	R	S	C_o	Δa (in.)	r_y	a_e	NU1 KI(a_e)max (ksi√in)
0	0		14.01	10.15	3.87	0.72	2.30	4.51E-10	2.93E-06	0.013		14.73
1	75		14.02	10.15	3.87	0.72	2.30	4.51E-10	2.93E-06	0.013		14.73
2	150		14.02	10.15	3.87	0.72	2.30	4.51E-10	2.93E-06	0.013		14.73
3	225		14.02	10.15	3.87	0.72	2.30	4.51E-10	2.93E-06	0.013		14.73
4	300		14.02	10.15	3.87	0.72	2.30	4.51E-10	2.93E-06	0.013		14.73
5	375		14.02	10.15	3.87	0.72	2.30	4.51E-10	2.93E-06	0.013		14.73
6	450		14.02	10.15	3.87	0.72	2.30	4.51E-10	2.94E-06	0.013		14.73
7	525		14.02	10.15	3.87	0.72	2.30	4.51E-10	2.94E-06	0.013		14.73
8	600		14.02	10.16	3.87	0.72	2.30	4.51E-10	2.94E-06	0.013		14.74
9	675		14.02	10.16	3.87	0.72	2.30	4.51E-10	2.94E-06	0.013		14.74
10	750		14.03	10.16	3.87	0.72	2.30	4.51E-10	2.94E-06	0.013		14.74
11	825		14.03	10.16	3.87	0.72	2.30	4.51E-10	2.94E-06	0.013		14.74
12	900		14.03	10.16	3.87	0.72	2.30	4.51E-10	2.94E-06	0.013		14.74
13	975		14.03	10.16	3.87	0.72	2.30	4.51E-10	2.94E-06	0.013		14.74
14	1050		14.03	10.16	3.87	0.72	2.30	4.51E-10	2.94E-06	0.013		14.74
15	1125		14.03	10.16	3.87	0.72	2.30	4.51E-10	2.94E-06	0.013		14.74
16	1200		14.03	10.16	3.87	0.72	2.30	4.51E-10	2.94E-06	0.013		14.74
17	1275		14.03	10.16	3.87	0.72	2.30	4.51E-10	2.95E-06	0.013		14.75
18	1350		14.04	10.16	3.87	0.72	2.30	4.51E-10	2.95E-06	0.013		14.75
19	1425		14.04	10.16	3.87	0.72	2.30	4.51E-10	2.95E-06	0.013		14.75
20	1500		14.04	10.17	3.87	0.72	2.30	4.51E-10	2.95E-06	0.013		14.75
21	1575		14.04	10.17	3.87	0.72	2.30	4.51E-10	2.95E-06	0.013		14.75
22	1650		14.04	10.17	3.87	0.72	2.30	4.51E-10	2.95E-06	0.013		14.75
23	1725		14.04	10.17	3.87	0.72	2.30	4.51E-10	2.95E-06	0.013		14.75
24	1800		14.04	10.17	3.87	0.72	2.30	4.51E-10	2.95E-06	0.013		14.75
25	1875		14.04	10.17	3.87	0.72	2.30	4.51E-10	2.95E-06	0.013		14.76

Table 10. Evaluation of an External Axial Flaw for Fatigue Crack Growth Along Path 2 (Cont'd)

AXIAL FLAW FATIGUE CRACK GROWTH FOR REMAINING TRANSIENTS

Basis: $\Delta a = \Delta N * C_o(\Delta KI)^n$

Transient frequency: 2760 cycles over 40 years

ΔN = 69 cycles/year

Operating Time (yr.)	Cycle	a (in.)	NU1 KI(a)max (ksi√in)	NU2 KI(a)min (ksi√in)	ΔKI (ksi√in)	R	S	C_o	Δa (in.)	r_y	a_e	NU1 KI(a_e)max (ksi√in)
0	0		15.02	8.66	6.35	0.58	2.04	3.99E-10	1.23E-05	0.015		15.91
1	69		15.02	8.66	6.36	0.58	2.04	3.99E-10	1.23E-05	0.015		15.91
2	138		15.02	8.66	6.36	0.58	2.04	3.99E-10	1.23E-05	0.015		15.91
3	207		15.02	8.66	6.36	0.58	2.04	3.99E-10	1.23E-05	0.015		15.91
4	276		15.02	8.66	6.36	0.58	2.04	3.99E-10	1.23E-05	0.015		15.91
5	345		15.02	8.66	6.36	0.58	2.04	3.99E-10	1.23E-05	0.015		15.91
6	414		15.02	8.67	6.36	0.58	2.04	3.99E-10	1.23E-05	0.015		15.92
7	483		15.02	8.67	6.36	0.58	2.04	3.99E-10	1.23E-05	0.015		15.92
8	552		15.03	8.67	6.36	0.58	2.04	3.99E-10	1.23E-05	0.015		15.92
9	621		15.03	8.67	6.36	0.58	2.04	3.99E-10	1.23E-05	0.015		15.92
10	690		15.03	8.67	6.36	0.58	2.04	3.99E-10	1.23E-05	0.015		15.92
11	759		15.03	8.67	6.36	0.58	2.04	3.99E-10	1.23E-05	0.015		15.92
12	828		15.03	8.67	6.36	0.58	2.04	3.99E-10	1.23E-05	0.015		15.92
13	897		15.03	8.67	6.36	0.58	2.04	3.99E-10	1.23E-05	0.015		15.92
14	966		15.03	8.67	6.36	0.58	2.04	3.99E-10	1.24E-05	0.015		15.93
15	1035		15.03	8.67	6.36	0.58	2.04	3.99E-10	1.24E-05	0.015		15.93
16	1104		15.04	8.67	6.36	0.58	2.04	3.99E-10	1.24E-05	0.015		15.93
17	1173		15.04	8.67	6.36	0.58	2.04	3.99E-10	1.24E-05	0.015		15.93
18	1242		15.04	8.67	6.36	0.58	2.04	3.99E-10	1.24E-05	0.015		15.93
19	1311		15.04	8.67	6.37	0.58	2.04	3.99E-10	1.24E-05	0.015		15.93
20	1380		15.04	8.68	6.37	0.58	2.04	3.99E-10	1.24E-05	0.015		15.93
21	1449		15.04	8.68	6.37	0.58	2.04	3.99E-10	1.24E-05	0.015		15.93
22	1518		15.04	8.68	6.37	0.58	2.04	3.99E-10	1.24E-05	0.015		15.94
23	1587		15.04	8.68	6.37	0.58	2.04	3.99E-10	1.24E-05	0.015		15.94
24	1656		15.05	8.68	6.37	0.58	2.04	3.99E-10	1.24E-05	0.015		15.94
25	1725		15.05	8.68	6.37	0.58	2.04	3.99E-10	1.24E-05	0.015		15.94

Table 11. Evaluation of a Continuous Surface Crack for Fatigue Crack Growth Along Path 4

INPUT DATA

Geometry:	Plate thickness,	t =	0.981	in.
Flaw Size:	Flaw depth,	a = [ ]		in.
		a/t = [ ]		
Environment:	Temperature,	T =	600	F
Material Strength:	Yield strength,	σ_{ys} =	27.9	ksi

Table 11. Evaluation of a Continuous Surface Crack for Fatigue Crack Growth Along Path 4 (Cont'd)

PLATE SURFACE FLAW STRESS INTENSITY FACTOR FOR HEATUP AND COOLDOWN STRESSES

Basis: Analysis of Flaws, 1995 ASME Code, Section XI, Appendix A (Ref. 16)

$$KI = [A_0 G_0 + A_1 G_1 + A_2 G_2 + A_3 G_3] \sqrt{(\pi a/Q)}$$

where $Q = 1 + 4.593*(a/l)^{1.65} - q_y$

and $q_y = [(A_0 G_0 + A_1 G_1 + A_2 G_2 + A_3 G_3) / \sigma_{ys}]^2 / 6$

For a/l = 0.0 (continuous flaw)
a/t <= 0.1

Go = 1.1945
G_1 = 0.7732
G_2 = 0.5996
G_3 = 0.5012

Stresses are described by a third order polynomial fit over the flaw depth,

$$S(x) = A_0 + A_1(x/a) + A_2(x/a)^2 + A_3(x/a)^3$$

Radial Stresses:

Wall Position x	Normal/Upset Cond. Stresses [6]	
	SS*	Shutdown
(in.)	(ksi)	(ksi)
0.00000		
0.24535		
0.49070		
0.73604		
0.98139		

* Heatup/Cooldown transient at 6.0 hours (steady state) using stresses for Path 4

Stress Coefficients: a = [ ] in.

Stress Coeff.	Normal/Upset Loading Conditions	
	NU1	NU2
	(ksi)	(ksi)
A_0		
A_1		
A_2		
A_3		

Table 11. Evaluation of a Continuous Surface Crack for Fatigue Crack Growth Along Path 4 (Cont'd)

PLATE SURFACE FLAW STRESS INTENSITY FACTOR FOR PLANT LOADING AND UNLOADING STRESSES

Basis: Analysis of Flaws, 1995 ASME Code, Section XI, Appendix A (Ref. 16)

$$KI = [A_0 G_0 + A_1 G_1 + A_2 G_2 + A_3 G_3] \sqrt{(\pi a/Q)}$$

where $Q = 1 + 4.593*(a/l)^{1.65} - q_y$

and $q_y = [(A_0 G_0 + A_1 G_1 + A_2 G_2 + A_3 G_3) / \sigma_{ys}]^2 / 6$

For a/l = 0.0 (continuous flaw)
a/t <= 0.1

Go = 1.1945
G_1 = 0.7732
G_2 = 0.5996
G_3 = 0.5012

Stresses are described by a third order polynomial fit over the flaw depth,

$$S(x) = A_0 + A_1(x/a) + A_2(x/a)^2 + A_3(x/a)^3$$

Radial Stresses:

Wall Position x	Normal/Upset Cond. Stresses [6]	
	PU*	PL**
(in.)	(ksi)	(ksi)
0.00000		
0.24535		
0.49070		
0.73604		
0.98139		

* Plant Loading/Unloading transient at 3.333 hours (plant unloading) using stresses for Path 4

** Plant Loading/Unloading transient at 0.333 hours (plant loading) using stresses for Path 4

Stress Coefficients: a = [ ] in.

Stress Coeff.	Normal/Upset Loading Conditions	
	NU1	NU2
	(ksi)	(ksi)
A_0		
A_1		
A_2		
A_3		

Table 11. Evaluation of a Continuous Surface Crack for Fatigue Crack Growth Along Path 4 (Cont'd)

PLATE SURFACE FLAW STRESS INTENSITY FACTOR FOR REMAINING TRANSIENT STRESSES

Basis: Analysis of Flaws, 1995 ASME Code, Section XI, Appendix A (Ref. 16)

$$KI = [\, A_0 G_0 + A_1 G_1 + A_2 G_2 + A_3 G_3 \,] \sqrt{(\pi a/Q)}$$

where $Q = 1 + 4.593*(a/l)\text{^}1.65 - q_y$

and $q_y = [\, (A_0 G_0 + A_1 G_1 + A_2 G_2 + A_3 G_3) / \sigma_{ys} \,]^2 / 6$

For a/l = 0.0 (continuous flaw)
a/t <= 0.1

G_o = 1.1945
G_1 = 0.7732
G_2 = 0.5996
G_3 = 0.5012

Stresses are described by a third order polynomial fit over the flaw depth,

$$S(x) = A_0 + A_1(x/a) + A_2(x/a)^2 + A_3(x/a)^3$$

Radial Stresses:

Wall Position x	Normal/Upset Cond. Stresses [6]	
	LL1*	LL2**
(in.)	(ksi)	(ksi)
0.00000		
0.24535		
0.49070		
0.73604		
0.98139		

* Loss of Load transient at 0.00278 hours (max. stress) using stresses for Path 4

** Loss of Load transient at 0.0444 hours (min. stress) using stresses for Path 4

Stress Coefficients: a = [ ] in.

Stress Coeff.	Normal/Upset Loading Conditions	
	NU1	NU2
	(ksi)	(ksi)
A_0		
A_1		
A_2		
A_3		

Table 11. Evaluation of a Continuous Surface Crack for Fatigue Crack Growth Along Path 4 (Cont'd)

CONTINUOUS SURFACE FLAW FATIGUE CRACK GROWTH FOR HEATUP AND COOLDOWN TRANSIENT

Basis: $\Delta a = \Delta N * C_o(\Delta KI)^n$

Transient frequency: 200 cycles over 40 years

ΔN = 5 cycles/year

Operating Time (yr.)	Cycle	a (in.)	Q	NU1 KI(a)max (ksi√in)	NU2 KI(a)min (ksi√in)	ΔKI (ksi√in)	R	S	C_o	Δa (in.)	q_y	$Q(a_e)$	$KI(a_e)max$ (ksi√in)
0	0		1.000	17.32	0.00	17.32	0.00	1.00	1.96E-10	1.20E-05	0.204	0.796	19.42
1	5		1.000	17.32	0.00	17.32	0.00	1.00	1.96E-10	1.20E-05	0.204	0.796	19.42
2	10		1.000	17.33	0.00	17.33	0.00	1.00	1.96E-10	1.20E-05	0.204	0.796	19.43
3	15		1.000	17.33	0.00	17.33	0.00	1.00	1.96E-10	1.20E-05	0.204	0.796	19.43
4	20		1.000	17.33	0.00	17.33	0.00	1.00	1.96E-10	1.20E-05	0.204	0.796	19.43
5	25		1.000	17.34	0.00	17.34	0.00	1.00	1.96E-10	1.20E-05	0.204	0.796	19.44
6	30		1.000	17.34	0.00	17.34	0.00	1.00	1.96E-10	1.20E-05	0.204	0.796	19.44
7	35		1.000	17.34	0.00	17.34	0.00	1.00	1.96E-10	1.20E-05	0.204	0.796	19.44
8	40		1.000	17.34	0.00	17.34	0.00	1.00	1.96E-10	1.20E-05	0.204	0.796	19.45
9	45		1.000	17.35	0.00	17.35	0.00	1.00	1.96E-10	1.20E-05	0.204	0.796	19.45
10	50		1.000	17.35	0.00	17.35	0.00	1.00	1.96E-10	1.20E-05	0.204	0.796	19.45
11	55		1.000	17.35	0.00	17.35	0.00	1.00	1.96E-10	1.20E-05	0.204	0.796	19.46
12	60		1.000	17.36	0.00	17.36	0.00	1.00	1.96E-10	1.20E-05	0.204	0.796	19.46
13	65		1.000	17.36	0.00	17.36	0.00	1.00	1.96E-10	1.21E-05	0.204	0.796	19.46
14	70		1.000	17.36	0.00	17.36	0.00	1.00	1.96E-10	1.21E-05	0.204	0.796	19.47
15	75		1.000	17.37	0.00	17.37	0.00	1.00	1.96E-10	1.21E-05	0.204	0.796	19.47
16	80		1.000	17.37	0.00	17.37	0.00	1.00	1.96E-10	1.21E-05	0.204	0.796	19.47
17	85		1.000	17.37	0.00	17.37	0.00	1.00	1.96E-10	1.21E-05	0.204	0.796	19.48
18	90		1.000	17.38	0.00	17.38	0.00	1.00	1.96E-10	1.21E-05	0.204	0.796	19.48
19	95		1.000	17.38	0.00	17.38	0.00	1.00	1.96E-10	1.21E-05	0.204	0.796	19.48
20	100		1.000	17.38	0.00	17.38	0.00	1.00	1.96E-10	1.21E-05	0.204	0.796	19.49
21	105		1.000	17.38	0.00	17.38	0.00	1.00	1.96E-10	1.21E-05	0.204	0.796	19.49
22	110		1.000	17.39	0.00	17.39	0.00	1.00	1.96E-10	1.21E-05	0.204	0.796	19.49
23	115		1.000	17.39	0.00	17.39	0.00	1.00	1.96E-10	1.21E-05	0.204	0.796	19.50
24	120		1.000	17.39	0.00	17.39	0.00	1.00	1.96E-10	1.21E-05	0.204	0.796	19.50
25	125		1.000	17.40	0.00	17.40	0.00	1.00	1.96E-10	1.21E-05	0.204	0.796	19.50

Table 11. Evaluation of a Continuous Surface Crack for Fatigue Crack Growth Along Path 4 (Cont'd)

CONTINUOUS SURFACE FLAW FATIGUE CRACK GROWTH FOR PLANT LOADING AND UNLOADING TRANSIENT

Basis: $\Delta a = \Delta N * C_o(\Delta KI)^n$

Transient frequency: 3000 cycles over 40 years

ΔN = 75 cycles/year

Operating Time (yr.)	Cycle	a (in.)	Q	NU1 KI(a)max (ksi√in)	NU2 KI(a)min (ksi√in)	ΔKI (ksi√in)	R	S	C_o	Δa (in.)	q_y	$Q(a_e)$	$KI(a_e)max$ (ksi√in)
0	0		1.000	18.25	12.08	6.17	0.66	2.19	4.29E-10	1.30E-05	0.227	0.773	20.76
1	75		1.000	18.25	12.09	6.17	0.66	2.19	4.29E-10	1.30E-05	0.227	0.773	20.76
2	150		1.000	18.26	12.09	6.17	0.66	2.19	4.29E-10	1.30E-05	0.227	0.773	20.77
3	225		1.000	18.26	12.09	6.17	0.66	2.19	4.29E-10	1.31E-05	0.227	0.773	20.77
4	300		1.000	18.26	12.09	6.17	0.66	2.19	4.29E-10	1.31E-05	0.227	0.773	20.77
5	375		1.000	18.27	12.09	6.17	0.66	2.19	4.29E-10	1.31E-05	0.227	0.773	20.78
6	450		1.000	18.27	12.10	6.17	0.66	2.19	4.29E-10	1.31E-05	0.227	0.773	20.78
7	525		1.000	18.27	12.10	6.18	0.66	2.19	4.29E-10	1.31E-05	0.227	0.773	20.78
8	600		1.000	18.28	12.10	6.18	0.66	2.19	4.29E-10	1.31E-05	0.227	0.773	20.79
9	675		1.000	18.28	12.10	6.18	0.66	2.19	4.29E-10	1.31E-05	0.227	0.773	20.79
10	750		1.000	18.28	12.10	6.18	0.66	2.19	4.29E-10	1.31E-05	0.227	0.773	20.80
11	825		1.000	18.29	12.11	6.18	0.66	2.19	4.29E-10	1.31E-05	0.227	0.773	20.80
12	900		1.000	18.29	12.11	6.18	0.66	2.19	4.29E-10	1.31E-05	0.227	0.773	20.80
13	975		1.000	18.29	12.11	6.18	0.66	2.19	4.29E-10	1.31E-05	0.227	0.773	20.81
14	1050		1.000	18.30	12.11	6.18	0.66	2.19	4.29E-10	1.31E-05	0.227	0.773	20.81
15	1125		1.000	18.30	12.12	6.18	0.66	2.19	4.29E-10	1.31E-05	0.227	0.773	20.81
16	1200		1.000	18.30	12.12	6.19	0.66	2.19	4.29E-10	1.32E-05	0.227	0.773	20.82
17	1275		1.000	18.31	12.12	6.19	0.66	2.19	4.29E-10	1.32E-05	0.227	0.773	20.82
18	1350		1.000	18.31	12.12	6.19	0.66	2.19	4.29E-10	1.32E-05	0.227	0.773	20.83
19	1425		1.000	18.31	12.12	6.19	0.66	2.19	4.29E-10	1.32E-05	0.227	0.773	20.83
20	1500		1.000	18.32	12.13	6.19	0.66	2.19	4.29E-10	1.32E-05	0.227	0.773	20.83
21	1575		1.000	18.32	12.13	6.19	0.66	2.19	4.29E-10	1.32E-05	0.227	0.773	20.84
22	1650		1.000	18.32	12.13	6.19	0.66	2.19	4.29E-10	1.32E-05	0.227	0.773	20.84
23	1725		1.000	18.33	12.13	6.19	0.66	2.19	4.29E-10	1.32E-05	0.227	0.773	20.84
24	1800		1.000	18.33	12.13	6.19	0.66	2.19	4.29E-10	1.32E-05	0.227	0.773	20.85
25	1875		1.000	18.33	12.14	6.20	0.66	2.19	4.29E-10	1.32E-05	0.227	0.773	20.85

Table 11. Evaluation of a Continuous Surface Crack for Fatigue Crack Growth Along Path 4 (Cont'd)

CONTINUOUS SURFACE FLAW FATIGUE CRACK GROWTH FOR REMAINING TRANSIENTS

Basis: $\Delta a = \Delta N * C_o(\Delta KI)^n$

Transient frequency: 2760 cycles over 40 years

ΔN = 69 cycles/year

Operating Time (yr.)	Cycle	a (in.)	Q	NU1 KI(a)max (ksi√in)	NU2 KI(a)min (ksi√in)	ΔKI (ksi√in)	R	S	C_o	Δa (in.)	q_y	$Q(a_e)$	$KI(a_e)max$ (ksi√in)
0	0		1.000	18.17	12.31	5.87	0.68	2.22	4.34E-10	1.03E-05	0.225	0.775	20.64
1	69		1.000	18.17	12.31	5.87	0.68	2.22	4.34E-10	1.03E-05	0.225	0.775	20.64
2	138		1.000	18.18	12.31	5.87	0.68	2.22	4.34E-10	1.03E-05	0.225	0.775	20.65
3	207		1.000	18.18	12.31	5.87	0.68	2.22	4.34E-10	1.03E-05	0.225	0.775	20.65
4	276		1.000	18.18	12.31	5.87	0.68	2.22	4.34E-10	1.03E-05	0.225	0.775	20.66
5	345		1.000	18.19	12.32	5.87	0.68	2.22	4.34E-10	1.03E-05	0.225	0.775	20.66
6	414		1.000	18.19	12.32	5.87	0.68	2.22	4.34E-10	1.03E-05	0.225	0.775	20.66
7	483		1.000	18.19	12.32	5.87	0.68	2.22	4.34E-10	1.03E-05	0.225	0.775	20.67
8	552		1.000	18.20	12.32	5.87	0.68	2.22	4.34E-10	1.03E-05	0.225	0.775	20.67
9	621		1.000	18.20	12.33	5.87	0.68	2.22	4.34E-10	1.03E-05	0.225	0.775	20.67
10	690		1.000	18.20	12.33	5.88	0.68	2.22	4.34E-10	1.03E-05	0.225	0.775	20.68
11	759		1.000	18.21	12.33	5.88	0.68	2.22	4.34E-10	1.03E-05	0.225	0.775	20.68
12	828		1.000	18.21	12.33	5.88	0.68	2.22	4.34E-10	1.04E-05	0.225	0.775	20.69
13	897		1.000	18.21	12.33	5.88	0.68	2.22	4.34E-10	1.04E-05	0.225	0.775	20.69
14	966		1.000	18.22	12.34	5.88	0.68	2.22	4.34E-10	1.04E-05	0.225	0.775	20.69
15	1035		1.000	18.22	12.34	5.88	0.68	2.22	4.34E-10	1.04E-05	0.225	0.775	20.70
16	1104		1.000	18.22	12.34	5.88	0.68	2.22	4.34E-10	1.04E-05	0.225	0.775	20.70
17	1173		1.000	18.23	12.34	5.88	0.68	2.22	4.34E-10	1.04E-05	0.225	0.775	20.70
18	1242		1.000	18.23	12.35	5.88	0.68	2.22	4.34E-10	1.04E-05	0.225	0.775	20.71
19	1311		1.000	18.23	12.35	5.88	0.68	2.22	4.34E-10	1.04E-05	0.225	0.775	20.71
20	1380		1.000	18.24	12.35	5.89	0.68	2.22	4.34E-10	1.04E-05	0.225	0.775	20.71
21	1449		1.000	18.24	12.35	5.89	0.68	2.22	4.34E-10	1.04E-05	0.225	0.775	20.72
22	1518		1.000	18.24	12.35	5.89	0.68	2.22	4.34E-10	1.04E-05	0.225	0.775	20.72
23	1587		1.000	18.25	12.36	5.89	0.68	2.22	4.34E-10	1.04E-05	0.225	0.775	20.73
24	1656		1.000	18.25	12.36	5.89	0.68	2.22	4.34E-10	1.04E-05	0.225	0.775	20.73
25	1725		1.000	18.25	12.36	5.89	0.68	2.22	4.34E-10	1.04E-05	0.225	0.775	20.73

9.0 SUMMARY OF RESULTS

The flaw evaluation results for 25 years of fatigue crack growth are as follows.

9.1 Propagation of a Continuous External Circumferential Flaw Along Path 2

a) Fatigue crack growth analysis:

Initial flaw size,	a_i = [ ] in.
Final flaw size,	a_f = [ ] in.
Stress intensity factor at final flaw size,	$K_I (a_{ef})$ = 17.9 ksi$\sqrt{in}$
Fracture toughness	K_{Ia} = 200 ksi$\sqrt{in}$
Fracture toughness margin,	K_{Ia} / K_I = 11.2 > $\sqrt{10}$

b) Limit load analysis:

Limit load,	P_O = [ ] lbs
Bounding axial tube load,	P(appl) = [ ] lbs
Limit load margin,	P_O / P(appl) = 8.47 > 3.0

9.2 Fatigue Crack Growth of a Semi-Circular External Axial Flaw Along Path 2

Initial flaw size,	a_i = [ ] in.
Final flaw size,	a_f = [ ] in.
Stress intensity factor at final flaw size,	$K_I (a_{ef})$ = 15.9 ksi$\sqrt{in}$
Fracture toughness	K_{Ia} = 200 ksi$\sqrt{in}$
Fracture toughness margin,	K_{Ia} / K_I = 12.6 > $\sqrt{10}$

9.3 Fatigue Crack Growth of a Continuous Cylindrical Flaw Along Path 4

Initial flaw size,	a_i = [ ] in.
Final flaw size,	a_f = [ ] in.
Stress intensity factor at final flaw size,	$K_I (a_{ef})$ = 20.9 ksi$\sqrt{in}$
Fracture toughness	K_{Ia} = 200 ksi$\sqrt{in}$
Fracture toughness margin,	K_{Ia} / K_I = 9.57 > $\sqrt{10}$

10.0 CONCLUSION

The results of the analysis demonstrate that the [ ] inch weld anomaly is acceptable for a 25 year design life of the CRDM ID temper bead weld repair. Significant fracture toughness margins have been demonstrated for both of the flaw propagation paths considered in the analysis. The minimum fracture toughness margins for flaw propagation Paths 2 and 4 have been shown to be 11.2 and 9.57, respectively, as compared to the required margin of $\sqrt{10}$ for normal and upset operating conditions per Section XI, IWB-3612 (Reference 3). Fatigue crack growth is minimal. The maximum final flaw size is [ ] inch (considering both flaw propagation paths). A limit load analysis was also performed considering the ductile Alloy 600/Alloy [ ] materials along flaw propagation Path 2. The analysis showed limit load margin of 8.47 for normal and upset operating conditions, as compared to the required margin of 3.0 per Section XI, IWB-3642 (Reference 3).

11.0 REFERENCES

1. Framatome ANP Drawing 02-5019702E-2, "Point Beach Unit 1 CRDM Nozzle ID Temper Bead Weld Repair."

2. Framatome ANP Document 51-5017195-05, "Point Beach 1 & 2 CRDM Nozzle ID Temper Bead Weld Repair Requirements," September 2002.

3. ASME Boiler and Pressure Vessel Code, Section XI, Rules for Inservice Inspection of Nuclear Power Plant Components, 1998 Edition with Addenda through 2000.

4. Welding Research Council, Bulletin No. 175, "PVRC Recommendations on Toughness Requirements for Ferritic Materials," New York, August 1972.

5. Framatome ANP Document 51-5012728-03, "Weld Anomaly Considerations in the CRDM ID Temper Bead Weld Repair," October 2001.

6. Framatome ANP Document 32-5020244-01, "Point Beach 1 CRDM Temperbead Bore Weld Analysis," February 2003.

7. ASME Section II, Part C, "Specification for Welding Rods, Electrodes, and Filler Metals," 1999 Addenda.

8. Framatome ANP Document 38-1288355-00, "Flaw Acceptance Criteria."

9. ASME Boiler and Pressure Vessel Code, Section III, Rules for Construction of Nuclear Power Plant Components, Division 1 - Appendices, 1989 Edition with No Addenda.

10. I.S. Raju and J.C. Newman Jr., "Stress Intensity Factors for Internal and External Surface Cracks in Cylindrical Vessels," Transactions of the ASME, Journal of Pressure Vessel Technology, pp. 293-298, Vol. 104, November 1982.

11. T.L. Anderson, Fracture Mechanics: Fundamentals and Applications, CRC Press, 1991.

12. W.J. Mills, "Fracture Toughness of Two Ni-Fe-Cr Alloys," Hanford Engineering Development Laboratory Document HEDL-SA-3309, April 1985.

13. C.B. Buchalet and W.H. Bamford, "Stress Intensity Factor Solutions for Continuous Surface Flaws in Reactor Pressure Vessels," Mechanics of Crack Growth, ASTM STP 590, American Society for Testing and Materials, 1976, pp. 385-402.

14. EPRI Topical Report, EPRI NP-1931, "An Engineering Approach for Elastic-Plastic Fracture Analysis," Research Project 1237-1, prepared by V. Kumar et al of General Electric Company, July 1981.

15. General Electric Report, SRD-82-048, "Estimation Technique for the Prediction of Elastic-Plastic Fracture of Structural Components of Nuclear Systems," by V. Kumar et al, Contract RP1237-1, Combined Fifth and Sixth Semi-Annual Report, March 1982.